Available online at www.sciencedirect.com
SCIENCE DIRECT®
Journal of Nuclear Materials 337–339 (2005) 327–331
journal of nuclear materials
www.elsevier.com/locate/jnucmat

Simulation of plasma fluxes to material surfaces with self-consistent edge turbulence and transport for tokamaks

T.D. Rognlien *, M.V. Umansky, X.Q. Xu, R.H. Cohen, L.L. LoDestro

University of California, Lawrence Livermore National Laboratory, P.O. Box 808, L-630, 7000 East Ave., Livermore, CA 94551, USA

Abstract

The edge-plasma profiles and fluxes to the divertor and walls of a tokamak with a magnetic X-point are simulated by coupling a 2D transport code (UEDGE) and a 3D turbulence code (BOUT). A relaxed iterative coupling scheme is used where each code is run on its characteristic time scale, resulting in a statistical steady state. Plasma variables of density, parallel velocity, and separate ion and electron temperatures are included, together with a fluid neutral model for recycling neutrals at material surfaces. Results for the DIII-D tokamak parameters show that the turbulence is preferentially excited in the outer radial region of the edge where magnetic curvature is destabilizing, yielding substantial plasma particle flux to the main chamber walls. The coupled transport/turbulence simulation technique provides a strategy to achieve physics-based predictions for future device performance.

PACS: 52.40.Hf; 52.35.Ra; 52.25.Fi; 52.65.−y
Keywords: Plasma turbulence; Edge transport; Non-diffusive transport; Neutral transport simulation; UEDGE

1. Introduction

The distribution of plasma fluxes to material surfaces is a key issue for fusion devices because it identifies peak heat loads, and determines hydrogenic and impurity particle sources from recycling and sputtering. The wall fluxes can erode the material, setting its lifetime, and release potentially undesirable impurities into the plasma discharge. The typical modeling approach for tokamaks has been to simulate the scrape-off layer (SOL) plasma with 2D transport codes that assume enhanced turbulence-induced transport across the magnetic field, **B**, to fit experimental profiles. Plasma turbulence simulations for fixed profiles, e.g., Ref. [1], show that turbulent fluxes of the required magnitude arise from instabilities driven by radial plasma gradients. However, because the profiles and turbulence are strongly coupled, predicting plasma fluxes in future devices such as ITER requires coupling of simulations for turbulence and profile evolution. The approach reported here is coupling the BOUT 3D turbulence code [1] with the UEDGE 2D transport code [2]. Initial coupling of only the plasma density variable for fixed temperature profiles is presented in [3]. A simpler 2D slab model of SOL turbulence driven by magnetic curvature described in Ref. [4] also includes evolution of the density profile for constant electron temperature. For the present paper, the coupling is extended to the electron and ion temperatures and the parallel velocity in toroidal tokamak geometry. Neutrals are treated self-consistently via a flux-limited fluid model with parallel inertia.

* Corresponding author. Tel.: +1 925 422 9830; fax: +1 925 423 3484.
E-mail address: trognlien@llnl.gov (T.D. Rognlien).

0022-3115/$ - see front matter © 2004 Elsevier B.V. All rights reserved.
doi:10.1016/j.jnucmat.2004.10.023

One feature of our simulations is a strong outward convection of the plasma in the far scrape-off layer. Such behavior has been observed or inferred by various diagnostics, such as Langmuir probes, Gas-Puff imaging, and imaging of background H_α light ([5,6] and references therein). Analysis of polarization of plasma density 'blobs' from opposite ion and electron ∇B drifts, and the resulting $\mathbf{E}\times\mathbf{B}$ drift, provides a simple explanation of the rapid outward motion [7]. However, understanding the growth and saturation of 'blobs,' as well as more complex dynamics, requires full turbulence simulations, e.g., Refs. [1,4]. The impact of large SOL edge-plasma transport has been analyzed previously by the empirical approach of fitting transport coefficients to those deduced from experimental data [8–10].

The approach taken here is to determine the transport by coupling with a 3D turbulence simulation that includes both closed and open B-field line regions near the magnetic separatrix. The combined model thus includes the generation of the 'blobs' from plasma turbulence, and the cross-B-field transport and particle recycling. Because the characteristic time scales of the turbulence is short and the profile evolution time scale can be long (owing to recycling), an efficient iterative scheme [11] is used that relaxes the turbulent fluxes passed from BOUT to UEDGE and the profiles from UEDGE to BOUT over many coupling steps. Each code is run on its own characteristic time scale, yielding a statistically averaged steady state. Since the turbulent fluxes are coupled directly to UEDGE with no assumption of small-amplitude diffusive transport, the effects of convective transport events are included.

The paper presents the models and coupling procedure in Section 2, gives results applied to DIII-D in Section 3, and provides a discussion and summary in Section 4.

2. Transport and turbulence models and coupling

The model for the edge plasma is taken from the strongly magnetized fluid equations of Braginskii [12] with some reductions as described in Refs. [1,2]. The 2D UEDGE and 3D BOUT codes use the common poloidal/radial mesh shown in Fig. 1 based on magnetic flux surfaces. The turbulence code includes a segment of the toroidal dimension. UEDGE evolves the primary toroidally averaged variables denoted by uppercase letters; namely, plasma and neutral densities ($N_{i,n}$), parallel ion and velocities ($V_{\|i,n}$), and electron and ion temperatures ($T_{e,i}$). The electrostatic potential (Φ) comes from the inertialess parallel electron momentum equation.

BOUT evolves fluctuating quantities with zero toroidal average, which are denoted as lower-case variables. For the electrostatic limit used here, there are six fluctuating field quantities: n_i, $v_{\|i}$, $v_{\|e}$, ϕ, t_e, and t_i, where electron momentum and vorticity equations are included. The turbulence has various drive mechanisms, including the destabilizing combination of magnetic curvature and radial plasma gradients on the outside of the torus, and the negative sheath resistance of the divertor plate sheath [1]. It is assumed that neutrals do not have a direct impact on the plasma turbulence, but can have an indirect effect via profile changes. For now, we suppress the turbulence in the private flux region. Characteristics of the edge turbulence are discussed in a separate paper at this conference [13].

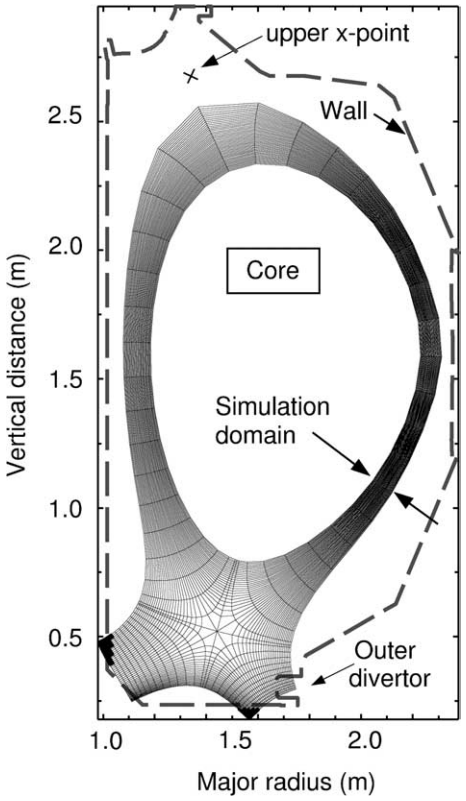

Fig. 1. Poloidal/radial simulation domain and mesh (64×50) for BOUT/UEDGE coupled simulation of DIII-D discharge 107404.

The transport equations are of the form of a convection–diffusion system

$$\frac{\partial \Psi_k}{\partial t} + \nabla\cdot(\mathbf{V}_k\Psi_k - D_k\nabla\Psi_k) = S_k, \tag{1}$$

where Ψ_k denote different plasma and neutral variables given above. The source/sink represent processes like ionization, recombination, energy loss, and also pressure work terms for the energy equations [2]. Standard edge-plasma boundary conditions are applied, where we fix the plasma variables at the core boundary. Specified particle recycling occurs at the divertor plates and outer

wall, where energy transmission coefficients provide temperature boundary conditions.

The coupling follows the procedure in Ref. [3] using toroidal and temporal averages of the BOUT radial fluxes, $\Gamma_{rk} = \langle \psi_k v_r \rangle$. Here the turbulent radial velocity is determined by the fluctuating $\mathbf{E}\times\mathbf{B}$ velocity, $v_r = -\nabla_2\phi/B$, where ∇_2 denotes the derivative in the direction normal to both $\mathbf{B}$ and the normal to the magnetic flux surface (radial). These fluxes are then used to define V_{rk} and D_{rk} within UEDGE to yield a consistent flux, i.e.

$$\Gamma_{rk} = V_{rk}\Psi_k - D_{rk}\nabla_r\Psi_k. \tag{2}$$

This separation into convective and diffusive components avoids negative D_{rk} and improves numerical stability. For the energy equations, the 'source terms' also involve nonlinear averages of turbulent quantities [e.g., $v_r \mathrm{d}(n_i t_i)/\mathrm{d}r$]. The fluxes in the parallel direction (along $\mathbf{B}$) are taken as classical [12] with flux limits.

The coupling between the transport and turbulence is accomplished through an iterative scheme of the type described in Refs. [3,11]. The total plasma variable ($=\Psi_k + \psi_k$) is the sum of the slowly evolving, toroidally averaged density and the faster fluctuation density. For the slow transport density, we solve

$$\frac{\partial \Psi_k^m}{\partial t} + \nabla\cdot(\mathbf{V}_{\|i}^m \Psi_k^m + \Gamma_{rk}^{m-1}) = S_k^m, \tag{3}$$

where m is the iteration index, and the flux Γ_{rk}^{m-1} comes from an average of previous turbulence iterations [3]. Likewise, the profiles used for the turbulence simulations are averaged over previous transport iterations.

Here, we couple plasma fluxes from BOUT for the density, and electron and ion temperatures, i.e., a particle flux and energy fluxes, thus extending the results given in Ref. [3]. In addition, we include the convection of the parallel momentum density ($m_i V_{\|}\langle n_i v_r\rangle$) due to the particle flux. We compute, but do not yet couple, the momentum flux $m_i\langle v_{\|i} v_r\rangle$. Likewise, some energy equation pressure terms are yet to be coupled.

3. Resulting plasma/neutrals profiles and wall fluxes

A coupled simulation is performed for DIII-D discharge 107404 as shown in Fig. 1. The core boundary ion density and temperatures are fixed to $N_i = 2.5\times10^{19}\,\mathrm{m}^{-3}$ and $T_e = T_i = 200\,\mathrm{eV}$. The plate recycling coefficient is 0.95 and that at the walls is 0.90 to model some pumping. Temperature boundary conditions at the plates and walls give electron (ion) energy flux of $4T_e$ ($2.5T_i$) times the particle flux.

The simulation is initiated from a plasma density profile generated in Ref. [3] for fixed temperature profiles to obtain fluxes from BOUT, where in addition to the poloidal/radial mesh of 64×50 shown in Fig. 1, 64 points are used for toroidal segment 1/30 of the total circumference. These fluxes are used to determine V_{rk} and D_{rk} from Eq. (2) in such a way that convection and diffusion contribute equally to the flux. The exception to the 50/50 split is that the minimum diffusion coefficient is set to $0.5\,\mathrm{m}^2/\mathrm{s}$ for N_i (and $0.25\,\mathrm{m}^2/\mathrm{s}$ for $T_{e,i}$), and the V_{rk} are then adjusted to give the correct total flux. These transport coefficients are used in UEDGE to calculate new plasma profiles. For each successive iteration between UEDGE and BOUT, 50% of the new flux and profiles is used for updating.

The convective component of midplane plasma fluxes after seven iterations is shown in Fig. 2. Here $\bar{V}_{rn} = 0.5\langle n_i v_r\rangle/N_i$ (with 50% of Γ_{rn} represented by D_{rn}) and similarly for $T_{e,i}$. There is a strongly increasing transport outside the separatrix for N_i that is qualitatively consistent with the notion of 'blob' propagation [7]. The small negative convection in some regions is typically the result of compensating for the minimum diffusion used. The convergence of the iteration procedure beyond iteration 7 is interrupted by the growth of large t_e fluctuations near the wall where t_e/T_e begins to exceed -1, a nonphysical limit, requiring improvements to the turbulence simulation. This problem applies to the far SOL region where the transport is already large, so the large outward transport there is unlikely to change.

The profiles of densities and temperatures at the outer midplane for iteration 7 are shown in Fig. 3. We also compare with a base-case that uses customary constant diffusion coefficients of $0.33\,\mathrm{m}^2/\mathrm{s}$ for density, and larger values for parallel momentum ($0.5\,\mathrm{m}^2/\mathrm{s}$) and plasma temperatures (1.0), resulting in about 1 MW power input from the core. The differences with strong convection are not so large, except for naturally longer scale lengths in the outer SOL, the T_e core profile, and the much larger neutral density.

Turning to the outer divertor plate, the profiles of particle and heat fluxes are compared in Fig. 4. Here the result with coupling to the turbulence code shows the impact of strong outward convection in the SOL by broadening both the particle and heat fluxes. The

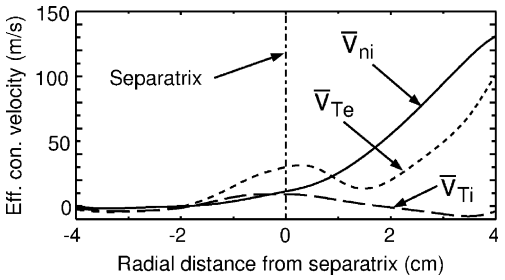

Fig. 2. Effective convective velocities at the outer midplane for density and temperatures from BOUT after seven iterations.

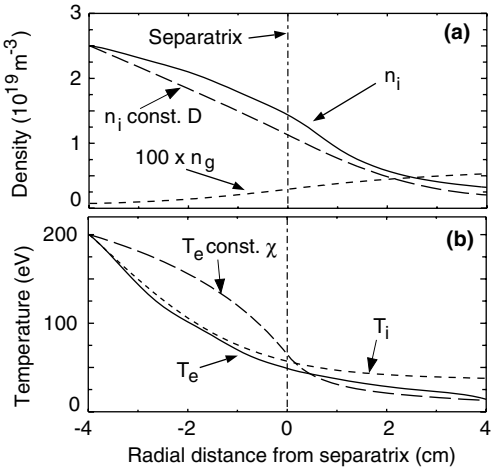

Fig. 3. Outer midplane profiles of (a) ion and neutral densities, and (b) temperatures at from UEDGE after seven iterations. The long-dash lines show results for N_i and T_e with constant diffusion.

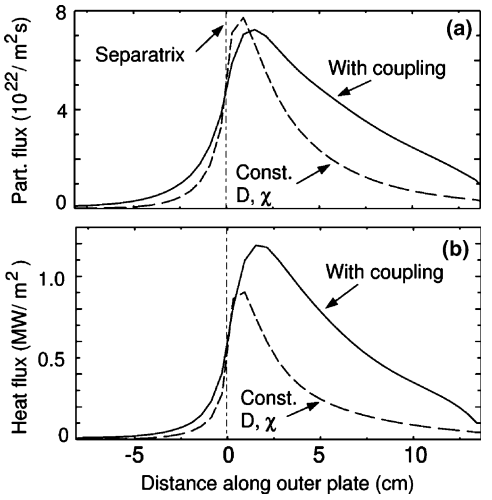

Fig. 4. Outer divertor plate profiles of (a) ion particle flux, and (b) heat flux comparing results with seven iterative BOUT/UEDGE couplings and the initial case with constant diffusion coefficients.

broadness of the profiles, especially near the separatrix, may be significantly affected by $\mathbf{E}\times\mathbf{B}$ shear stabilization of the turbulence not included in the simulations.

The impact of the self-consistent transport is seen most dramatically on the fluxes to the outer wall as shown in Fig. 5(a) and (b). There is both much larger wall flux for the coupled case, and the fluxes are focused on the outboard region of the SOL, between the upper X-point and the lower X-point (Fig. 1); such 'ballooning' character for the turbulence is expected from the unfavorable magnetic curvature on the outside of the torus [1]. While the upper X-point is not included in the simulation domain, its impact is felt through a minimum in the poloidal magnetic field, B_p, in this region. The peak of fluxes near the upper X-point is partially caused by the gradient of the turbulence scaling as $\nabla_2 \sim 1/B_p$, such that $v_r = -\nabla_2\phi/B$ can become large there. In terms of global particle and power heat fluxes, the case considered shows that the wall particle and power fluxes are about 40% of those to the divertor plates; these ratios are similar because of the fortuitously similar wall and plate temperatures. The ion and neutral densities along the outer wall after the seventh iteration are shown in Fig. 5(c). The neutral density is a direct consequence of recycling from the large ion flux. Over the main chamber region on the outside of the torus, the neutral density is $\sim 10^2$ times that for the constant diffusion case. The peaks near each end are associated with divertor plate recycling.

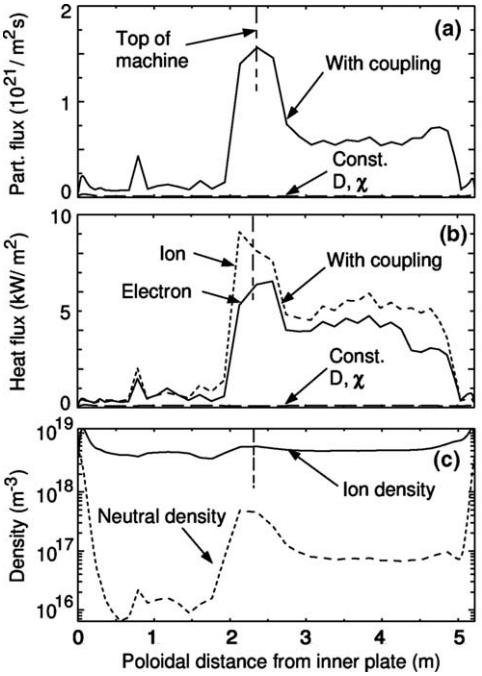

Fig. 5. Outer wall profiles of (a) ion particle flux and (b) heat flux comparing results after seven iterative BOUT/UEDGE couplings with results using constant diffusion coefficients. In (c), ion and neutral wall densities are shown corresponding to the seventh iterative coupling.

4. Summary

A method for obtaining a self-consistent model of edge-plasma turbulence and profiles is described. The algorithm couples 2D transport and 3D turbulence

simulations where each code is run on its own characteristic time scale. During each cycle of the iterative procedure, the toroidally averaged plasma profiles are evolved to steady state including particle recycling. A fraction of these profiles is used to update the profiles driving fluctuations in the 3D turbulence code. Likewise, a fractional update of the turbulent fluxes is provided to the transport code from the turbulence simulation.

The procedure is illustrated with a simulation for a DIII-D single-null configuration, and compared with a simple case having constant cross-field diffusion. The self-generated turbulence leads to strong radial transport in the far SOL, as inferred from some experimental diagnostics. About 40% of the particle and power flux go to the main chamber wall for the case simulated. While the coupling strategy appears to remain stable, the ultimate iterative convergence of this case is restricted by far SOL fluctuations eventually yielding negative T_e, requiring improvements to the turbulence simulation. A complementary procedure is to evolve the profiles on each turbulence time step [14]. While costly for times relevant to recycling-induced profile modifications, this method more accurately describes the influence of large, short-time profile adjustments to the turbulence.

Neutrals arising from recycling of the substantial ion flux to the chamber walls shown in Fig. 5 do have an influence on the plasma profiles and thus indirectly on plasma turbulence. Because the ionization rate is typically small compared to the turbulence growth rate, the neutrals are not included directly in the turbulence equations. An important issue for reactors is the charge-exchange sputtering caused by neutrals penetrating to higher T_i regions of the edge. The possible impact of these charge-exchange neutrals has been estimated for an ARIES-RS configuration in Ref. [10] with the conclusion that wall erosion rates could be much larger than previous estimates.

Acknowledgments

We thank S.I. Krasheninnikov, D.D. Ryutov, and D.G. Whyte for helpful discussions. This work was performed under the auspices of the US Department of Energy by the University of California Lawrence Livermore National Laboratory under contract No. W-7405-Eng-48 and was supported by LDRD project 03-ERD-009.

References

[1] X.Q. Xu, R.H. Cohen, T.D. Rognlien, J.R. Myra, Phys. Plasmas 7 (2000) 1951.
[2] T.D. Rognlien, D.D. Ryutov, N. Mattor, G.D. Porter, Phys. Plasmas 6 (1999) 1851.
[3] T.D. Rognlien, M.V. Umansky, X.Q. Xu, R.H. Cohen, Contrib. Plasma Phys. 44 (2004) 188.
[4] Y. Sarazin, Ph. Ghendrih, G. Attuel, et al., J. Nucl. Mater. 313–316 (2003) 796.
[5] B. LaBombard, M.V. Umansky, R.L. Boivin, et al., Nucl. Fusion 40 (2000) 2041.
[6] J.A. Boedo, D.L. Rudakov, R.A. Moyer, et al., Phys. Plasmas 10 (2003) 1670.
[7] S.I. Krasheninnikov, Phys. Lett. A 283 (2001) 368.
[8] M.V. Umansky, S.I. Krasheninnikov, B. LaBombard, et al., Phys. Plasmas 6 (1999) 2793.
[9] A.Yu. Pigarov, S.I. Krasheninnikov, T.D. Rognlien, et al., Contrib. Plasma Phys. 44 (2004) 228.
[10] M. Kotschenreuther, T.D. Rognlien, P. Valanju, Fusion Eng. Des. 72 (2004) 169.
[11] A.I. Shestakov, R.H. Cohen, J.A. Crotinger, L.L. LoDestro, A. Tarditi, X.Q. Xu, J. Comput. Phys. 185 (2003) 399.
[12] S.I. Braginskii, in: Leontovich M.A. (Ed.), Reviews of Plasma Physics, vol. 1, Consultants Bureau, New York, 1965, p. 205.
[13] M.V. Umansky, T.D. Rognlien, X.Q. Xu, these Proceedings, doi:10.1016/j.jnucmat.2004.10.021.
[14] X.Q. Xu, W.M. Nevins, R.H. Cohen, et al., Contrib. Plasma Phys. 44 (2004) 105.